Supplemental Figure 1

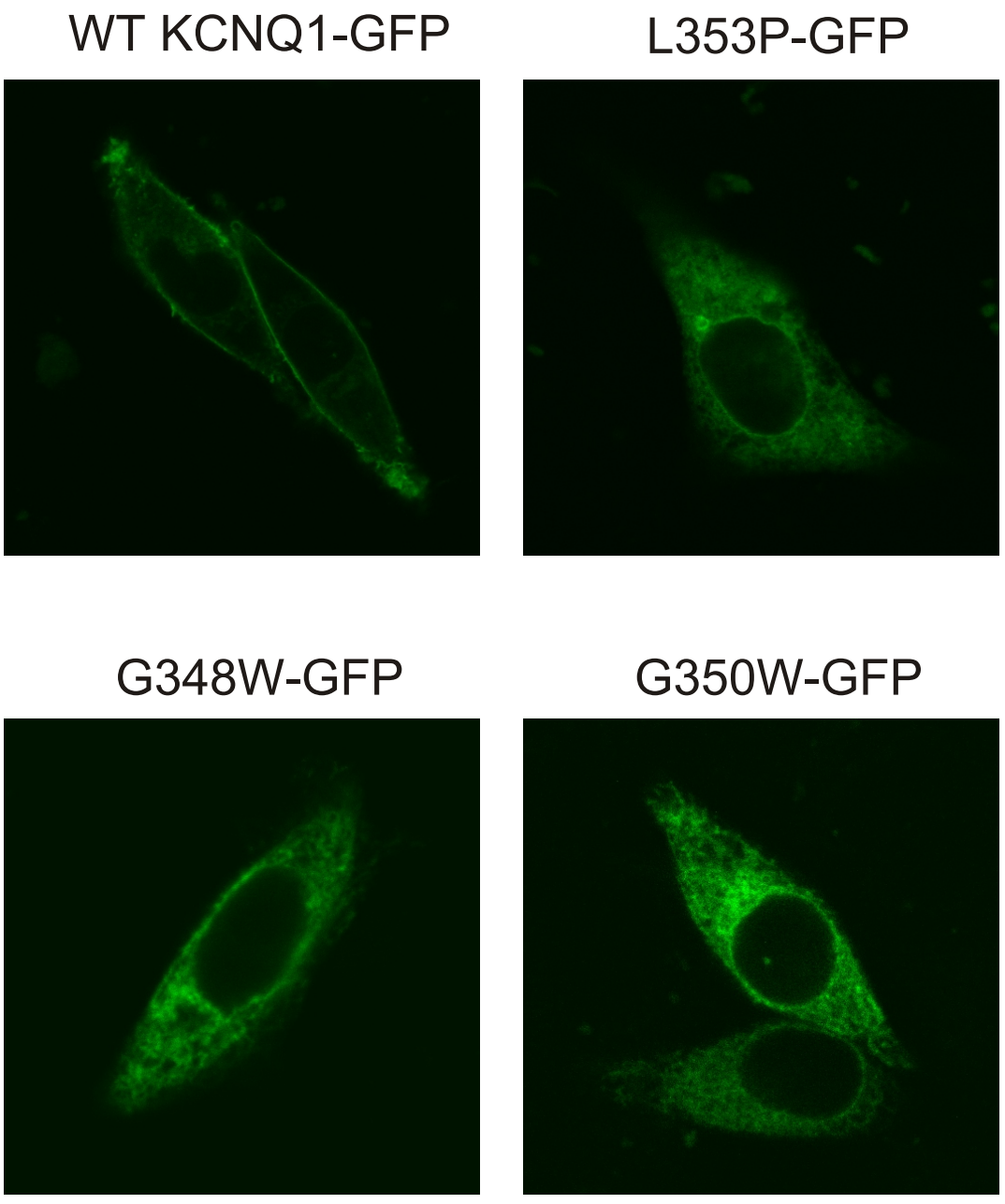

Supplemental Figure 2

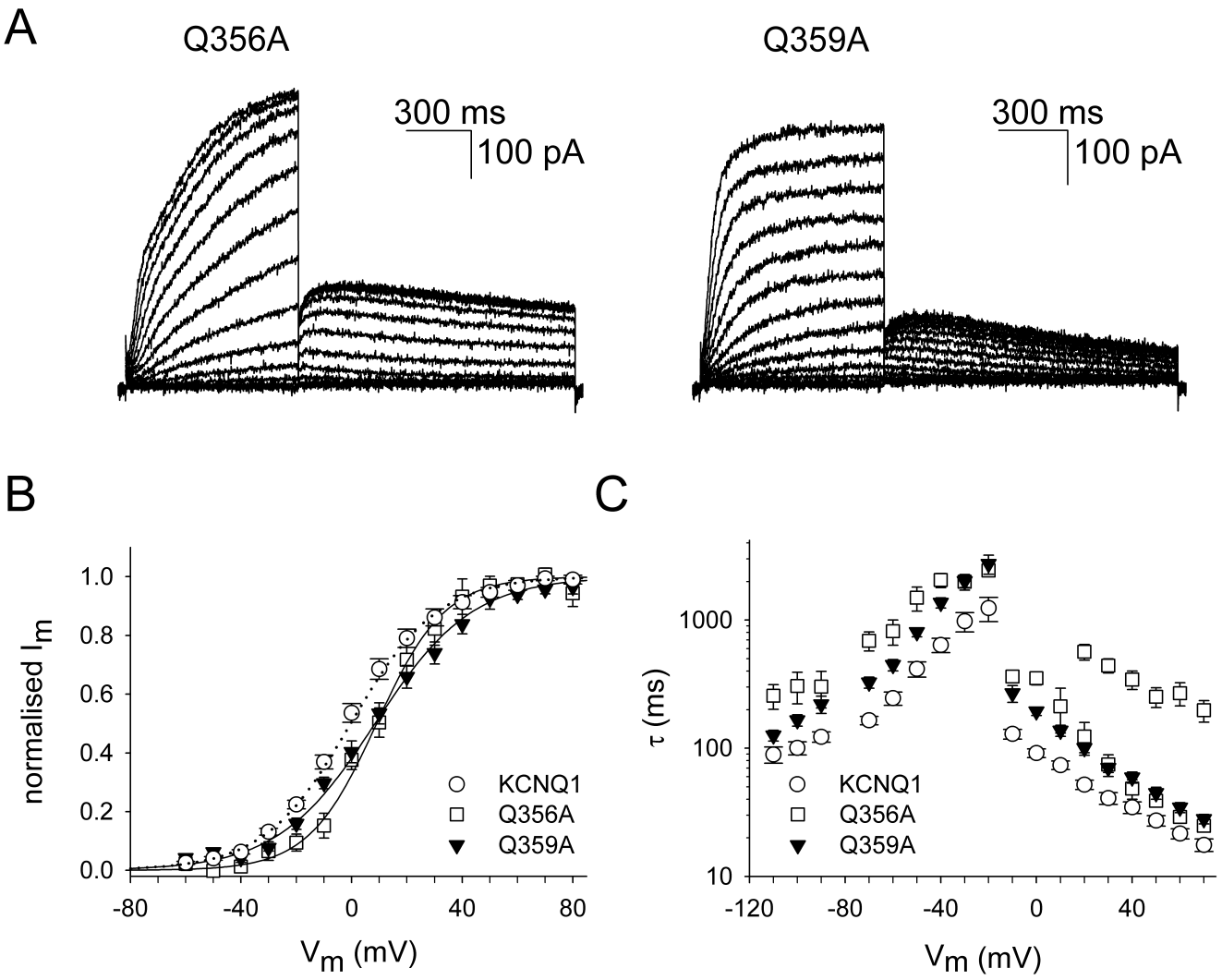

Supplemental Figure 3

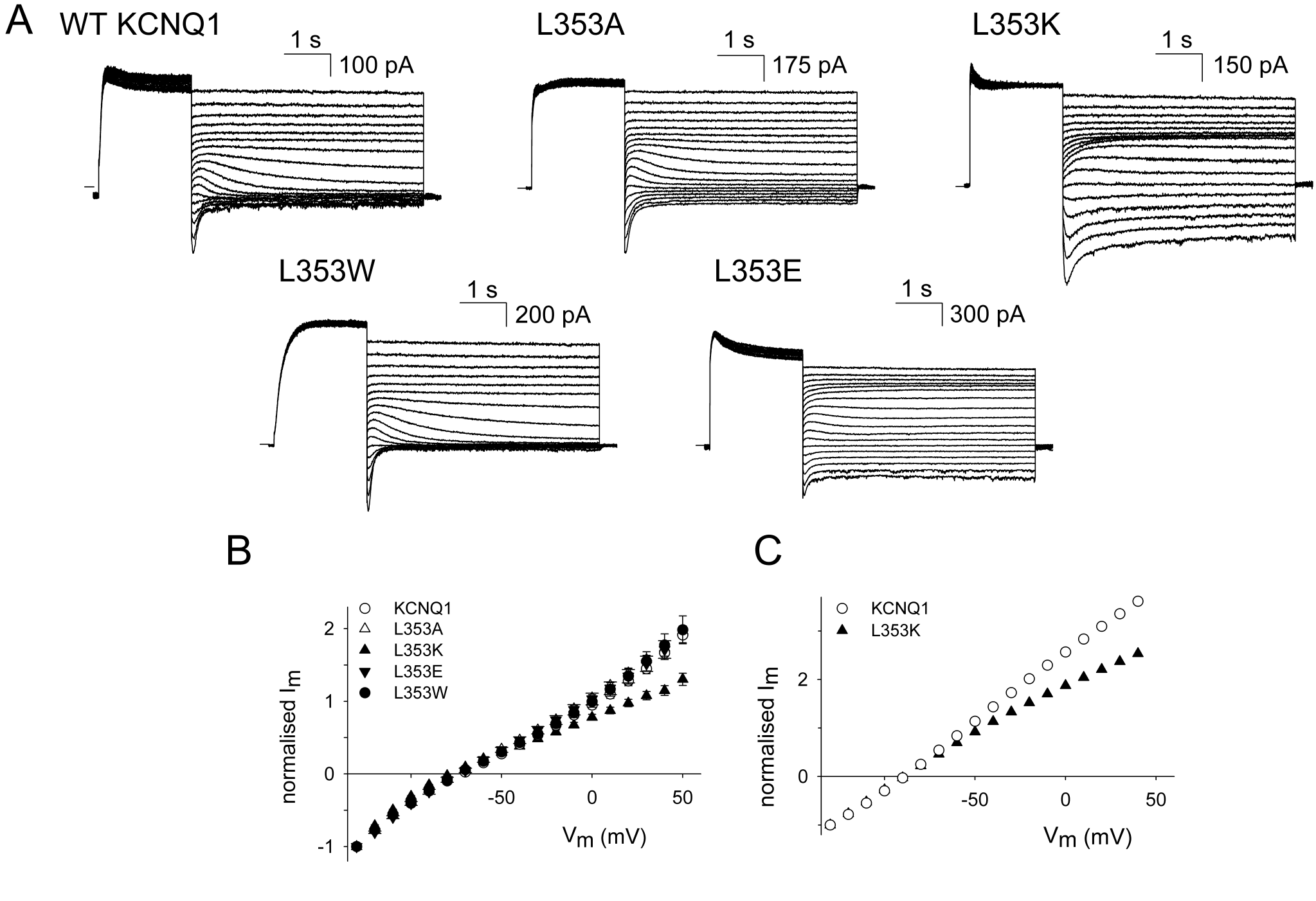

Supplemental Figure 4

A

96 mM Rb^+/ 100 mM K^+

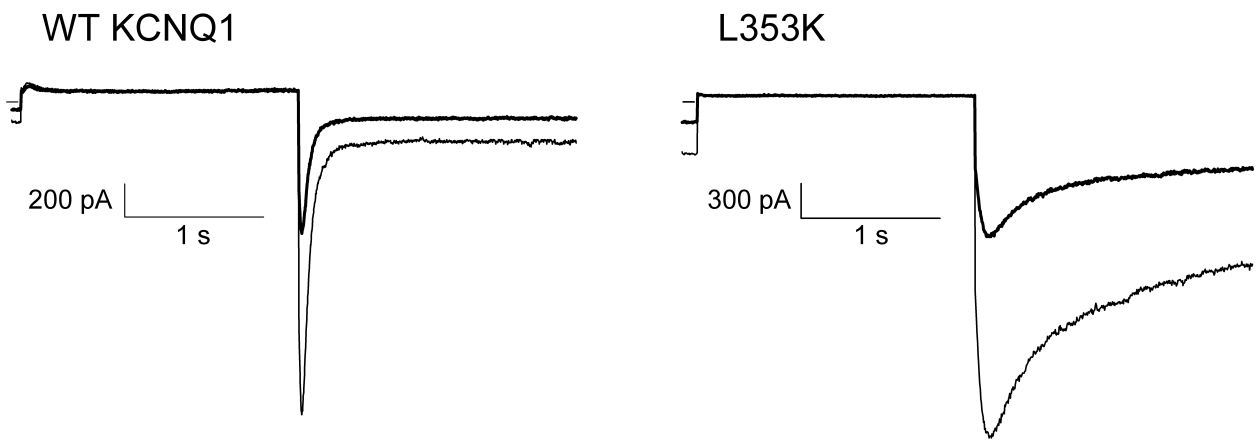

B

145 mM Rb^+/ 149 mM K^+

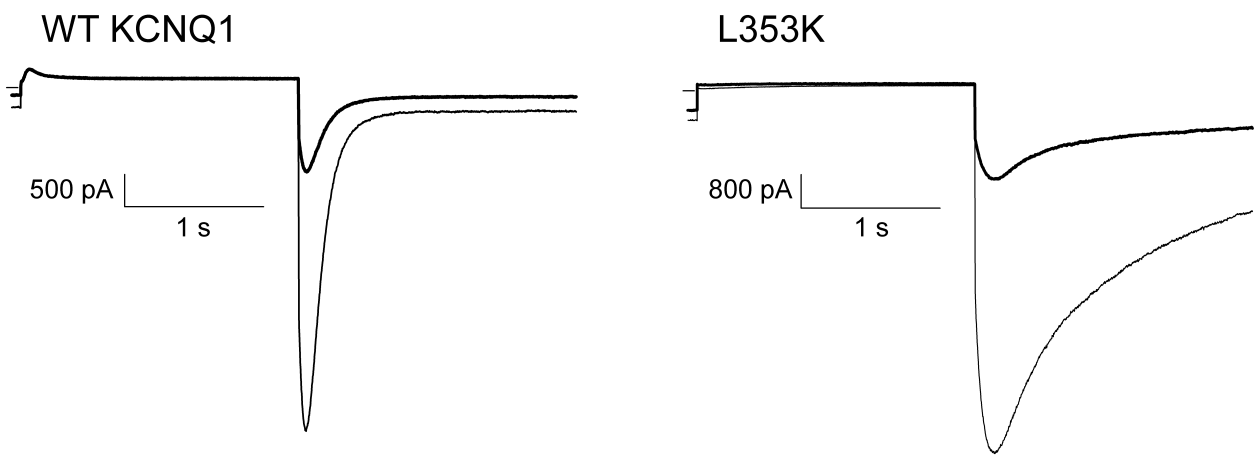

Supplemental data

Figure 1S: CHO-K1 cells were grown on cover slips and transfected using lipofectamine (Invitrogen). WT KCNQ1 and mutants were expressed in a pBK-CMV expression vector and tagged with GFP at the C-terminus. For transfection, 2 μg of WT KCNQ1-GFP or mutant KCNQ1-GFP cDNA was used. 48 hours after transfection, confocal images were obtained on a Zeiss CLSM 510, equipped with an argon laser (excitation, 488nm) for the visualisation of GFP. Note that the clear membrane localization of the WT KCNQ1 channels is not observed for the mutants.

Figure 2S: (A) Representative current traces for mutants Q356A and Q359A expressed in CHO-K1 cells. Cells were clamped at a holding potential of -80 mV and 800 ms pulses to voltages between -60 to +70 mV were imposed in steps of 10 mV. Tail currents were recorded by stepping to -40 mV. (B) Voltage dependence of activation. Activation curves were obtained by plotting the normalized tail currents as a function of the pre-pulse potential. The solid lines represent the average Boltzmann fit and were compared to WT (dotted line). For both mutants, no significant difference in voltage dependence of activation was observed. (C) Activation and deactivation time constants derived from mono-exponential and bi-exponential fits to the raw current traces were plotted as a function of the applied potential. Both mutants showed a slowing of the deactivation kinetics. The Q356A mutant showed a double exponential activation course.

Figure 3S: Fully activated (FA) I-V relationships for WT KCNQ1, L353A, L353K, L353E and L353W.

(A) Representative current traces for the WT KCNQ1 and mutants L353A, L353K, L353E and L353W. The cells were clamped at a holding potential of -80 mV, and a 2000 ms pulse to +50 mV was imposed. Tail currents were recorded from +40 mV to -130 mV in steps of -10 mV. Horizontal bar on the left indicates the zero current level. (B) FA I-V relationship for WT KCNQ1 (n = 8) and mutants L353A (n = 12), L353K (n = 11), L353E (n = 4) and L353W (n = 9). Currents were normalised to the amplitude at -130 mV. For the L353K mutant, the FA I-V relationship showed inward rectification. For WT KCNQ1, L353A,

L353E and L353W, the FA I-V relationship was quasi linear. (C) Simulations of the I-V relationships for WT KCNQ1 and the L353K mutant. The 4-barrier 3-site model of Peres-Cornejo et al was used with the energy maxima from the outside to the inside of the pore set at 4.4, 4, 4 and 6.7 RT (RT = 583 cal/mol) (Perez-Cornejo & Begenisich, 1994). The I-V relationship was quasi linear for WT KCNQ1. Inward rectification for the L353K mutation was simulated by increasing the inner barrier with 0.5 RT.

Figure 4S: (A) Representative current traces for WT KCNQ1 and L353K expressed in CHO-K1 cells elicited by a 2000 ms pulse to + 40 mV and a return to -120 mV. For the tail current analysis of the WT KCNQ1 and L353K mutant, a high $[K^+]_o$ (in mM, 100 KCl, 49 NaCl, 1.8 $CaCl_2$, 1 $MgCl_2$, 10 HEPES, 10 glucose, and adjusted to pH 7.35 with NaOH) and a high $[Rb^+]_o$ (in mM, 96 RbCl, 49 NaCl, 4 KCl, 1.8 $CaCl_2$, 1$MgCl_2$, 10 HEPES, 10 glucose, and adjusted to pH 7.35 with NaOH) solution were used. (B) Representative current traces for WT KCNQ1 and L353K expressed in CHO-K1 cells elicited by a 2000 ms pulse to +40 mV and a return to -90 mV. For the tail current analysis of the WT KCNQ1 and L353K mutant, a high $[K^+]_o$ (in mM, 149 KCl, 1.8 $CaCl_2$, 1 $MgCl_2$, 10 HEPES, 10 glucose, and adjusted to pH 7.35 with KOH) and a high $[Rb^+]_o$ (in mM, 145 RbCl, 4 KCl, 1.8 $CaCl_2$, 1 $MgCl_2$, 10 HEPES, 10 glucose, and adjusted to pH 7.35 with RbOH) solution were used. The relative Rb^+/K^+ conductance was determined from the ratio of the peak inward tail current I_{Rb}/I_K at (A) -120 mV and (B) -90 mV measured from the same cell bathed in the high $[Rb^+]_o$ or in the high $[K^+]_o$ solution in accordance to previous studies (Pusch *et al.*, 2000;Seebohm *et al.*, 2003). Currents recorded in high K^+ (thick trace) are overlayed with those recorded form the same cell bathed in high Rb^+ (thin trace). Horizontal bar at the left indicates the zero current level. The relative peak inward tail current amplitudes I_{Rb}/I_K at -120 mV in the extracellular solution containing 96 mM Rb^+ versus 100 mM K^+ (A) were 2.29 ± 0.07 (n = 6) and 2.34 ± 0.10 (n = 6) for WT KCNQ1 and L353K respectively. As the former solutions contained a remaining fraction of Na^+, these experiments were also performed in extracellular solutions containing 145 mM Rb^+ and 149 mM K^+ (B), to exclude any effect of Na^+, although it was indicated that Na^+ ions did not affect the inward tail currents (Pusch *et al.*, 2000). The relative peak inward tail current amplitudes at -90 mV in the latter solutions were: for WT KCNQ1: I_{Rb}/I_K = 4.3 ±

0.4 (n = 7), for L353K: I_{Rb}/I_K = 4.4 ± 0.3 (n = 6). The I_{Rb}/I_K ratio was similar for WT KCNQ1 and L353K under both conditions indicating that the L353K mutant demonstrates no significant difference in inactivation compared to WT KCNQ1 (Seebohm *et al.*, 2003).